Assembly of Long Chain Phosphatidylcholines at a Liquid–Liquid Interface

B. L. SMILEY, G. L. RICHMOND

Department of Chemistry, University of Oregon, Eugene, Oregon 97403

Received 3 May 1999; revised 29 June 1999; accepted 23 July 1999

ABSTRACT: The molecular-level organization of mixed and pure saturated symmetric chain 1,2-diacyl-*sn*-glycero-3-phosphocholines (PCs) adsorbed at a carbon tetrachloride–aqueous interface is explored by probing the hydrocarbon chain conformation within the adsorbed layer. PCs of the chain lengths found most frequently in biological systems, which in pure form are seen to form either very well-ordered or disordered layers, are observed in these studies to assemble into interfacial layers ranging from disordered to ordered states when mixed in various proportions. Independently, while C_{16} and shorter chain PCs tend to form disordered layers, a strong increase in ordering is observed for C_{18} and longer chain PCs in which the hydrocarbon chains are found to be primarily in an all trans conformation. Pure C_{17}-PCs adsorbed at the interface produce layers with an intermediate degree of chain ordering. The ability to tune interfacial layer properties in mixed systems as a function of molecular composition, including PC chain length as demonstrated here, is an important mechanism by which surface characteristics of oil–water emulsion systems can be controlled both *in vivo* and in numerous commercial applications. © 2000 John Wiley & Sons, Inc. Biopolymers (Biospectroscopy) 57: 117–125, 2000

Keywords: phospholipids; monolayers; vibrational spectroscopy; vibrational sum frequency spectroscopy; liquid surfaces

INTRODUCTION

Oil–water emulsions stabilized by interfacially adsorbed surfactants are utilized extensively in commercial processes and preparations. However, these emulsions also provide an available model system of particular interest to biologists because the oil–water interface between natural emulsion particles in the form of dietary fats and surrounding biological fluids plays a crucial role in metabolic processes.[1–3] The oil–water interface and the action of common natural surfactants such as phosphatidylcholines (PCs) within this unique environment have not been well characterized. PCs, commonly referred to as lecithins when present as a complex mixture of different hydrocarbon chain structures in food preparations, seem to have been characterized somewhat nonselectively in this context. Careful experimental investigations of PCs and other membrane phospholipids at an oil–water interface are sparse.[1,4–9] PCs as the majority component of membrane bilayers *in vivo* have been well studied, but adsorbed PC monolayers, which, for example, stabilize the surface of plasma lipoproteins in the blood in a manner dependent on the hydrocarbon chain composition of the adsorbed PCs,[10] have typically not been characterized, particularly at the molecular level of organization.

Correspondence to: G. L. Richmond (richmond@oregon.uoregon.edu).

Contract grant sponsor: National Science Foundation; contract grant number: CHE 9531402.

Contract grant sponsor: Office of Naval Research.

Biopolymers (Biospectroscopy), Vol. 57, 117–125 (2000)

© 2000 John Wiley & Sons, Inc.

The latter is due, at least in part, to a lack of suitable experimental techniques, although some theoretical models have been proposed.[11,12]

In the present investigations, we explore the molecular-level organization of saturated symmetric chain PCs adsorbed at the macroscopic interface between immiscible aqueous and carbon tetrachloride (CCl_4) phases utilizing a vibrational spectroscopic technique with an intrinsic specificity for surfaces. Average ordering within the adsorbed layers is deduced as a function of chain length based on the PC hydrocarbon chain conformation. We extend our previous investigations of PCs adsorbed at the liquid–liquid interface to include molecules with still longer hydrocarbon chains up to C_{22}, which could not be reasonably prepared by our previously described method[13] but are feasible with the method described herein. The results show a strong increase in relative ordering for the longer chain PCs, including those with an odd number of carbons per chain. The chain ordering of selected mixtures of adsorbed PCs is seen to be composition dependent, indicative of natural structural variances present in the large variety of functional biological membrane assemblies suited to a multitude of roles. The trends observed in these studies are distinctly different from those that might be expected based on complimentary results obtained for more simple, nonbiological surfactants.

MATERIALS AND METHODS

Theory of Vibrational Sum Frequency Generation from Interfaces

Investigation of molecular ordering at buried interfaces, such as the liquid–liquid interface between CCl_4 and water, provides a particular experimental challenge to surface scientists. In the case of membrane lipids such as PC monolayers, a few thermodynamic characterizations based on surface tension measurements[1,7–9] and images generated by fluorescence microscopy[14,15] have provided only clues to the molecular-level ordering. On the theoretical side, computer modeling techniques have postulated possible molecular conformations.[11,12] Vibrational sum frequency generation (VSFG), used here to probe the acyl chain conformation of PCs adsorbed at the aqueous–CCl_4 interface, is a surface-specific vibrational spectroscopic technique that has demonstrated molecular specificity and the ability to probe surface conformations.

The interfacial specificity of SFG is derived from the symmetry constraints imposed on a second-order process that in this case is an optical process. Typically, when an electromagnetic field is incident on a material, a polarization, P, is induced within the material with a magnitude proportional to the magnitude of the electric field, E. However, sufficiently intense electric fields may produce higher order effects within the medium such that P is no longer a linear function of E. In SFG two intense laser beams at frequencies ω_1 and ω_2 are overlapped within a medium, thereby inducing a polarization at the sum of the two frequencies, $\omega_{SF} = \omega_1 + \omega_2$. The magnitude of the electric field generated at the sum frequency, E_{SF}, as represented in Eq. (1) is proportional to the product of the two incident electric fields and the second-order nonlinear susceptibility, $\overleftrightarrow{\chi}^{(2)}$, characteristic of the material.

$$E_{SF} \propto P_{SF} = \overleftrightarrow{\chi}^{(2)} E_{vis} E_{IR} \quad (1)$$

Using the widely applied electric dipole approximation, SFG is symmetry forbidden in isotropic materials including many bulk liquids but necessarily allowed at interfaces where inversion symmetry is broken. It is this break in symmetry that occurs at surfaces from which the interfacial specificity of SFG is derived. By this same argument the SF response is selective for orientationally ordered adsorbates at an interface even in the presence of unadsorbed, randomly ordered molecules in either bulk phase defining that interface. VSFG has been widely applied at many types of solid, liquid, and gas interfaces, including buried interfaces, because of this intrinsic surface specificity.[16–24]

The second-order nonlinear susceptibility tensor, $\overleftrightarrow{\chi}^{(2)}$, which characterizes the interface includes both resonant and nonresonant components. These VSFG measurements are sensitive to the resonant component of the susceptibility, $\overleftrightarrow{\chi}_R^{(2)}$, which is enhanced when one of the laser beams, in our case a tunable IR source, comes into resonance with allowed molecular vibrational transitions. The magnitude of the resonant response, given by $\overleftrightarrow{\chi}_R^{(2)} = N\langle\alpha^{(2)}\rangle$, is determined by the number of contributing oscillators, N, and an orientationally averaged distribution of the molecular hyperpolarizability, $\alpha^{(2)}$, for the particular

chemical group. The molecular hyperpolarizability, as defined in Eq. (2),[24]

$$\alpha^{(2)} = \sum_n \frac{A_n}{\omega_n - \omega_{IR} - i\Gamma_n} \quad (2)$$

is a sum over all molecular vibrational resonances n, where A_n is an amplitude term proportional to the product of the Raman and IR transition moments. A_n will be zero if either the Raman or IR transition moment is zero such that the particular molecular vibration must be both Raman and IR active to be SF active and contribute to the measured SF signal.[25] The ω_n in Eq. (2) is defined as the frequency of the particular molecular vibrational transition, ω_{IR} is the frequency of the tunable IR source, and Γ_n is the line width of the transition. When the IR source is tuned such that $\omega_{IR} = \omega_n$, $\alpha^{(2)}$ in the above expression becomes large. An additional several orders of magnitude signal enhancement was obtained in all of our VSFG measurements by using a total internal reflection geometry in which the generated SF response is emitted from the sample interface at the critical angle.[26–29]

Optical System

The pump laser for our VSF measurements is a Q-switched Nd:YAG laser producing 12-ns pulses at 10 Hz. The 1064-nm output of the pump laser is divided into two components, one of which is frequency doubled to produce the 532-nm visible beam directed into the sample cell. The remaining 1064-nm light generates IR light via a $LiNbO_3$ optical parametric oscillator tunable over the 3.2–3.7 μm range that is focused and directed at the sample interface overlapping the larger 532-nm beam spot at the interface. The visible and tunable IR sources are both incident on the interface from the more optically dense CCl_4 subphase in order to permit use of a total internal reflection geometry. This arrangement is also beneficial because the aqueous phase is strongly absorbing in the IR. The visible beam is incident at approximately its critical angle during alignment and is adjusted to maximize the generated VSF response. The SF signal is measured in reflection as a function of the incident IR frequency using a photomultiplier tube and gated detection electronics preceded by appropriate optical filters.

Sample Preparation

The deuterium oxide (D_2O, 99.9%, HPLC grade) used as the aqueous phase was obtained from Cambridge Isotope Laboratories (Andover, MA) and adjusted to pH 7.0 with a 10 m*M* phosphate buffer (Mallinckrodt). Carbon tetrachloride (CCl_4, 99.9%, HPLC grade) was from Sigma–Aldrich. All PCs had stated purities greater than 99% and were obtained in powered form (Avanti Polar Lipids, Alabaster, AL) and used as received. Chloroform ($CHCl_3$, 99+%, HPLC grade) containing 0.5–1% ethanol as a stabilizer was purchased from Sigma–Aldrich. Deuterated chloroform (99.8% D) was obtained fresh from Cambridge Isotope Laboratories. All glassware and the sample cells were cleaned by soaking in Nochromix reagent (Fisher) followed by thorough rinsing with organic-free water from a Nanopure filtration system (Barnstead), drying in an oven, and cooling to room temperature prior to use.

Sample cells were prepared with D_2O buffer added on top of the CCl_4 subphase to form a complete overlayer. D_2O was used as the aqueous phase rather than H_2O in order to reduce adsorption of the IR pulse energy at the interface, which can cause boiling. The prepared sample cell was then allowed to sit for at least 2 h before spreading the PC dissolved in chloroform at a concentration between 1 and 2.5 mg/mL at the liquid–liquid interface by gently expelling small drops of the $CHCl_3$ solution from a syringe tip placed underneath the air–water interface, allowing them to fall by gravity to the liquid–liquid interface. Nonquantitative spreading of a portion of the PC dissolved in the $CHCl_3$ droplets then occurred at the liquid–liquid interface during dissolution of the $CHCl_3$ into the CCl_4 subphase. Typically for the longer chain PCs, two sample spreadings separated by at least an hour for the initial spreading solvent to dissipate from the interface were necessary to produce a close-packed interfacial layer at the liquid–liquid interface. Samples prepared using $CDCl_3$ as a spreading solvent were produced as described for samples spread from $CHCl_3$. PC stock solutions in $CDCl_3$ were placed in cold storage between uses and protected from exposure to light to inhibit degradation of the solvent (in the absence of stabilizer). Interfacial layers of mixed PCs were prepared by spreading a solution of mixed PCs dissolved in $CHCl_3$ in the manner described for the pure PC samples.

RESULTS AND DISCUSSION

Dependence of Ordering on Chain Length

VSF measurements of surfactants that select SF active vibrational modes with components normal to the liquid–liquid interface have been utilized to characterize the relative degree of ordering of component hydrocarbon chains.[13,22–24,30] This characterization was based on a comparison of the strength of the methyl (CH_3) versus methylene (CH_2) symmetric stretch (SS) modes. Because symmetry requirements necessitate that a vibrational mode be both IR and Raman allowed for SFG to occur at an interface, the CH_2-SS of well-ordered, all trans hydrocarbon chains within an adsorbed interfacial layer is SF inactive[31,32] and will not be observed in our measurements. By this argument, the CH_2-SS peak is small for well-ordered chains whether the chosen polarization combinations are selective for vibrational modes oriented either normal to or parallel to the interface. The CH_2 asymmetric stretch (AS) is also expected to be SF inactive for all trans hydrocarbon chains in a well-ordered monolayer.[31,32] In layers with disordered hydrocarbon chains, the symmetry requirements are relaxed and the CH_2-SS appears in the SF spectrum for modes both parallel and perpendicular to the interface. The trend for the CH_3-SS mode is opposite that of the CH_2-SS mode. In monolayers with well-ordered, all trans hydrocarbon chains, the CH_3 symmetry axes will be aligned in a narrow distribution near normal to the interface, producing a strong SF active CH_3-SS mode. In layers with disordered hydrocarbon chains, the distribution of orientations for the CH_3 symmetry axes is broader and, on average, will have an orientation with a much larger component parallel to the interface plane. Both these factors serve to reduce the CH_3-SS mode SF intensity normal to the interface in a disordered interfacial layer. We are therefore able to quantify the relative degree of chain ordering in our adsorbed PCs by comparison of the spectrally distinct CH_3-SS mode to CH_2-SS mode intensities normal to the interface plane within our SF spectra. The reduced number density of adsorbate molecules expected for a disordered interfacial layer serves to nonselectively reduce the observed SF intensity for all vibrational modes in the spectrum and should not impact the peak ratio.

The possibility of PC multilayer formation at an oil–water interface has been raised where PCs are adsorbed from the organic phase to the liquid–liquid interface[5,6] and also where adsorption occurs from the aqueous phase involving mechanical perturbation of the surface.[13] We do not assume that a single PC monolayer is present at the liquid–liquid interface in these studies. Whether monolayers or multilayers are formed at the liquid–liquid interface, which is perhaps dependent on the PC hydrocarbon chain length, only those layers that lack inversion symmetry will contribute to the SF signal intensity being measured.[33] SFG investigations of Langmuir–Blodgett multilayers in which successive monolayers on a substrate are oriented head to head and tail to tail suggest that the measured SF signal originates only from the top monolayer.[31] Although it is not certain from which layer within an adsorbed multilayer our SF response may originate if this structure is present, it is clear that distinct differences in the overall layer chain ordering are indicated by our measurements.

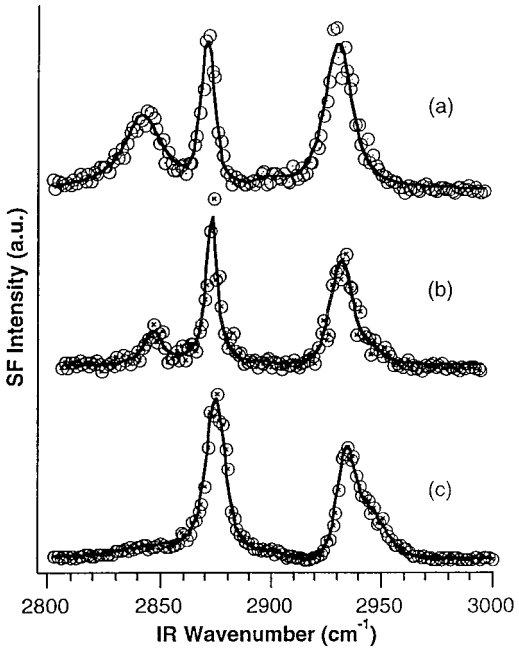

Figure 1. The measured SF intensity as a function of the incident IR wavenumber. Spectra are shown for (a) C_{16}-PC, (b) C_{17}-PC, and (c) C_{18}-PC adsorbed at the aqueous–CCl_4 interface for ssp polarization conditions. Lines are provided as a guide to the eye.

Figure 1 shows the SF data for s-polarized sum frequency, s-polarized visible, and p-polarized IR fields (i.e., ssp polarization conditions) giving the measured SF intensity as a function of wavenumber for the incident IR field. The data have been

normalized according to the incident IR intensity measured before the sample cell. In Figure 1(a) the spectrum for adsorbed 1,2-dipalmitoyl-*sn*-glycero-3-PC (C_{16}-PC) indicates disordered hydrocarbon chains evidenced by the presence of a strong CH_2-SS mode centered at approximately 2850 cm^{-1} and a relatively weak CH_3-SS mode centered near 2875 cm^{-1}. A peak centered at approximately 2932 cm^{-1} in this spectrum, which is included only for completeness and is not utilized in our analysis, is assigned to a methylene AS mode (CH_2-AS). A methylene Fermi resonance contribution (CH_2-FR) can be seen weakly near 2900 cm^{-1}. The shoulder at about 2945 cm^{-1} to the high energy side of the CH_2-AS is believed to arise from a methyl asymmetric stretch. Because of the spectral congestion in the region of the CH_2-AS we did not use this peak in the spectral analysis. However, we expect it to show intensity changes similar to the CH_2-SS mode with conformational order.

In comparison, the spectra given in Figure 1(b,c) for adsorbed 1,2-diheptadecanoyl-*sn*-glycero-3-PC (C_{17}-PC) and 1,2-distearoyl-*sn*-glycero-3-PC (C_{18}-PC) layers, respectively, show a relatively small CH_2-SS mode combined with a relatively strong CH_3-SS mode indicating well-ordered hydrocarbon chains. A similar pattern wherein a strong increase in chain ordering was observed for the C_{18}-PC compared to C_{16}- and shorter chain PCs was observed in samples adsorbed from aqueous PC suspensions to the CCl_4–aqueous interface in earlier studies.[13] These results are supported by published data obtained from electrochemical measurements of ion permeability for PCs of various chain lengths adsorbed at a polarized nitrobenzene–water interface in which symmetric chain PCs with 16 or fewer carbon atoms per chain formed liquid-expanded monolayers while those with 18 or more carbon atoms per chain formed monolayers present in a liquid-condensed state at the liquid–liquid interface.[4,5] The possibility for formation of PC multilayers at sufficient PC concentrations in the bulk nitrobenzene phase is also noted in this work.[5] Agreement between our results and those obtained at the nitrobenzene–water interface by PC adsorption from nitrobenzene[4,5] suggest that our spreading method may be complemented by adsorption of dissolved PCs from the CCl_4 phase that are not initially spread at the interface. The addition of PCs by spreading in $CHCl_3$ at the interface may produce a disproportionately high PC concentration in the vicinity of the liquid–liquid interface that subsequently enhances the rate of PC adsorption. X-ray scattering studies of multilamellar PC vesicles at room temperature have likewise indicated a decrease in the cross-sectional area occupied per chain with increasing chain length attributed to tighter chain packing.[34] It should also be noted that $CHCl_3$ is a known anesthetic, as are alcohols and CCl_4, although the latter as a nonpolar molecular species is significantly less potent.[35] It has been suggested in work investigating the mechanism of anesthetic action that the presence of adsorbed PCs at an interface enhances the interfacial concentration of the anesthetic relative to the neat interface.[36,37]

In order to more quantitatively gauge ordering of the PC hydrocarbon chains, a ratio of integrated intensities of the CH_3-SS peak to the CH_2-SS peak calculated from the measured ssp SF spectra was used. As mentioned above, the ratio of CH_3-SS/CH_2-SS will be large for well-ordered hydrocarbon chains and small for disordered chains. Experiments of Bell et al.[24] at the air–water interface on a variety of adsorbed surfactants obtained peak ratios between 10 and 0.8 for the most and least densely packed monolayers, respectively, as calculated from their ssp spectra. No phospholipid samples were included in the mentioned work. Well-ordered layers of adsorbed PCs at a liquid–liquid interface demonstrated somewhat lower maximum peak ratios,[13] possibly as a consequence of hydrophobic solvent interaction with the hydrocarbon chains. Our calculated peak ratios for adsorbed layers of C_{15}-PC through C_{22}-PC (including odd number chains) are shown in Figure 2 as a function of chain length. Consistent with the trend shown in Figure 1, it is clear that a large increase in ordering is observed for C_{17}- and longer chain PCs as compared to the C_{15} and C_{16}-PCs that possess a similar degree of disorder. The chains of the C_{18}- through C_{22}-PCs are all well-ordered to a similar extent, each exhibiting a very small CH_2-SS mode combined with a relatively large CH_3-SS mode as was shown for C_{18}-PC in Figure 1(c). The CH_2-SS peak in these spectra appears to attain a minimum size that is not reduced further at greater chain lengths. It is also noteworthy that ordering for PCs with an odd number of carbon atoms per acyl chain does not differ from the observed trend for the more physiologically relevant PCs with even numbers of carbons per chain. This similarity was also reported in thermodynamic data.[38] The increasing number of methylene units rela-

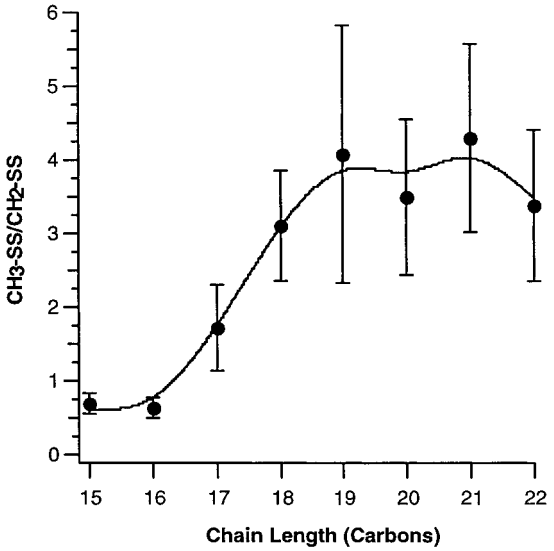

Figure 2. The calculated CH_3-SS/CH_2-SS peak ratios vs. PC chain length. Error bars are given based on the variance between multiple samples.

tive to methyl groups at greater chain lengths, which in disordered layers might be expected to increase the CH_2-SS mode intensity based simply on an increased number density of oscillators with increasing chain length, does not appear to be a factor in this trend. Rather, there appears to be a minimum thickness for the hydrophobic chain layer at which well-ordered layers can be formed. A similar trend was noted in previous work for layers of asymmetric and symmetric chain PCs at a liquid–liquid interface prepared by a different method.[13] It is interesting to note that the stable chain-packing structure of the saturated, symmetric, and fully hydrated PC gels changes in the chain length region of 18–20 carbons as the chain length is increased.[39,40] The shorter chain packing structure, which is the normal one, is described as disordered orthorhombic. The longer chain packing phase is significantly more ordered and very much resembles the orthorhombic perpendicular packing found for crystalline *n*-alkanes.

Nonquantitative spreading of the PC from $CHCl_3$ in the process of forming the adsorbed PC interfacial layers as noted has potential consequences in the interpretation of our SF data. Along the path of the incident IR beam in the sample cell CCl_4 phase prior to the sample spot, PCs dissolved in trace quantities in the CCl_4 subphase will selectively absorb energy near the CH_2-AS and CH_2-SS regions of the spectrum to a much greater extent than in the CH_3-SS region because of the much greater number of CH_2 groups present, although absorption peaks may be shifted from the SF intensity peaks. Subsequently, if IR absorption in the subphase by dissolved PCs is significant, the incident IR intensity near the CH_2 stretches will be selectively reduced. The measured SF CH_2-SS mode intensity, as represented in Eq. (1) by E_{SF}^2, would then be reduced relative to the CH_3-SS mode intensity, resulting in an inappropriately large CH_3-SS/CH_2-SS ratio. Final bulk PC concentrations in the CCl_4 phase were on the order of 10 μM in these experiments if we assume that bulk phase depletion resulting from interfacial adsorption is negligible. The latter is not necessarily a valid assumption for spread or partially spread layers at an interface where the relative proportion of surface-adsorbed molecules is significant. Given that PC solubility in CCl_4 should increase with increasing chain length and our data show an increase in ordering ratio with increasing PC chain length, the possible significance of this phenomenon was experimentally investigated.

Immediately prior to and after the sample cell, the IR intensity incident on a prepared C_{20}-PC sample and transmitted from the sample cell after total internal reflection from the liquid–liquid interface was measured as a function of frequency using a standard power meter. Assuming total reflection of the IR at the interface and equal path lengths into and out of the cell, the IR intensity at the sample spot was estimated to be intermediate between the incident and reflected beam intensities. Only slight dips in IR intensity were evident at approximately 2850 and 2930 cm^{-1} corresponding to absorbances from solution phase vibrational resonances of CH_2 SS and AS, respectively. A more gradual decrease in reflected IR intensity was observed below 2880 cm^{-1}, and a pronounced increase in IR absorption was observed above 2975 cm^{-1}. IR absorbance measurements of a CCl_4 sample taken from the cell subphase following the experiment identified the decreasing transmission below 2880 cm^{-1} as resulting from an absorption tail of D_2O monomers dissolved in the CCl_4. From the same measurement, the pronounced decrease in transmission above 2975 cm^{-1} can be attributed to an absorption tail from the CH vibrational resonance of the $CHCl_3$ spreading solvent, now dissolved in the CCl_4. Very small absorption peaks corresponding to CH_2 SS and AS vibrational resonances were observed overlapping the D_2O absorption tail and

appeared to be insignificant in comparison. These measurements indicate that specific subphase absorption of the tunable IR energy in the vicinity of the CH_2-SS is not responsible for the small SF peak intensity observed for this mode in the longer chain PCs. Rather, the hydrocarbon chains of these PCs appear, in fact, to be well ordered.

An additional consideration that may impact the ordering of the various adsorbed PCs is the presence of ethanol (as a manufacturer-added stabilizer) in the $CHCl_3$ spreading solvent. Ethanol has been shown to alter or increase the monolayer or bilayer structural properties, even in trace quantities, and may induce phase separations in mixed systems.[41] In anesthetic dosages, alcohols have also been shown to perturb hydration of the PC head group,[42] suggesting alterations in membrane structural properties. Because commercially available $CHCl_3$ is not available without stabilizer, we prepared spreading solutions of PCs dissolved in deuterated chloroform ($CDCl_3$), which is available without stabilizers and must be handled accordingly, for comparison with the $CHCl_3$ results. The chain ordering of PCs spread from $CDCl_3$ did not appear to differ significantly from those prepared with $CHCl_3$. The presence of ethanol in the spreading solvent therefore does not appear to be a factor in the observed ordering.

Mixed C_{16}- and C_{18}-PCs

If we now consider only physiologically relevant PCs with an even number of carbon atoms per chain, the position at which the transition from a disordered layer to an ordered layer occurs is between C_{16}-PC and C_{18}-PC as was shown in Figure 2. In biological membranes the PC alkyl chains are primarily composed of C_{16} and C_{18} chain lengths, C_{20} chains being the other significant portion.[43] If the length of the hydrocarbon chains can be related to structural stability of the interfacial layer, mixtures of "unstable" C_{16}- and "stable" C_{18}-PC chains could conceivably produce an intermediate degree of stability at the liquid–liquid interface. This intermediate degree of ordering between rigid inflexibility and random disorder is reflective of the pseudostability and complexity inherent in many biological systems. Although our SFG measurements were done *in situ* under ambient conditions (i.e., room temperature), it has been suggested in previous work that laser heating of the sample spot during SFG measurements under the specified experimental

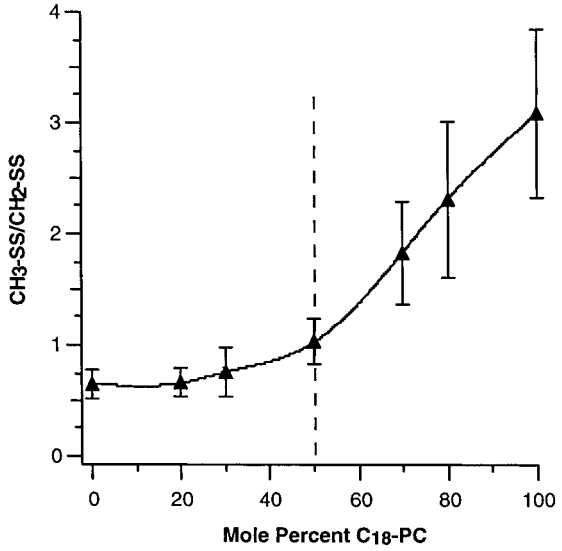

Figure 3. The CH_3-SS/CH_2-SS peak ratios calculated for various mole percent mixtures of C_{18}-PC with C_{16}-PC spread at the aqueous–CCl_4 interface. SF intensities were measured under ssp polarization conditions.

conditions may raise the local interface temperature to between 41 and 44°C.[13] While ordering of the interfacial layer is temperature dependent, the region of the adsorbed layer being sampled may actually be close to body temperature (37°C) and our results therefore applicable to *in vivo* comparisons.

Results from different mole percent mixtures of C_{16}-PC with C_{18}-PC at the liquid–liquid interface are summarized in Figure 3, where we are again using the CH_3-SS/CH_2-SS peak ratio calculated from SFG ssp spectra as a quantitative measure of hydrocarbon chain ordering. We assume that either the different chain length PCs mix close to homogeneously in the adsorbed layer or that sampling over time during SFG measurements is representative of the average chain ordering present within the layer. DSC measurements of C_{14}- and C_{16}-PC mixtures incorporated into multilamellar vesicles have indicated that mixing is not ideal and is less homogeneous with a larger mole fraction of the C_{16}-PC.[44] The calculated peak ratio obtained from VSFG measurements versus the mole percent of C_{18}-PC is shown in Figure 3. The data indicate that up to approximately 30% spread C_{18}-PC, the PC chains are as disordered as in a pure C_{16}-PC sample. At larger percentage C_{18}-PC compositions, chain ordering steadily increases until a well-ordered layer is obtained at greater than 80% spread C_{18}-PC. It is noteworthy

that at spread 50% C_{18}-PC/50% C_{16}-PC, the hydrocarbon chains are still relatively disordered rather than at the midpoint between ratios calculated for the two pure monolayers. In this 1:1 mixture the two methylene unit mismatch between neighboring C_{16}- and C_{18}-PC chains may still prohibit close chain packing. There are several other possible explanations for this, the most obvious being that our measure of the hydrocarbon chain ordering, the ratio of integrated intensities CH_3-SS/CH_2-SS, is a relative measure only and may not be a linear function of the chain ordering. The chain ordering also need not vary in a simple "linear" fashion as a function of composition. Experimentally, another factor that may play into the trend observed in Figure 3 is that the PCs when spread independently from $CHCl_3$ at the liquid–liquid interface appear to vary in their efficiency of spreading such that the final adsorbed layer composition at the interface may differ proportionately from the composition of the spreading solution. Nonideal mixing within the interfacial layer may also be a factor in some way. Other studies have noted that the rate of formation of a close-packed interfacial layer is slower with increasing chain length,[5] which is consistent with our observations. For PCs with hydrocarbon chain lengths greater than 19 carbon atoms, excess PCs from the second spreading were observed to produce flat, elliptical islands on top of the interfacial layer, which apparently results from an inability of PCs in the $CHCl_3$ droplets to penetrate the interface and thereby dissolve in the CCl_4 subphase. None of the PCs studied are soluble as monomers in the aqueous phase to a significant extent.

VSFG measurements incorporating chain-deuterated PCs were performed in an attempt to better elucidate the ordering of the particular PCs in the binary mixture and possibly glean information about the relative population of the two PCs adsorbed at the interface from the measured SF intensities. Experiments with mixed C_{16}- and C_{18}-PCs in which one or the other species was deuterated seemed to indicate in complimentary mixtures of *d*-C_{18}-PC/C_{16}-PC and C_{18}-PC/*d*-C_{16}-PC of the same molar ratio that the chain ordering, as deduced from the peak area ratio of VSFG ssp spectra, was smaller for both samples than for the peak ratio obtained in similar samples with only hydrogenated chains. Unfortunately, the signal intensities obtained for either one or the other hydrogenated species in the mixtures was too small relative to the noise level to provide for a reliable quantitative comparison. The small size of the generated signal results from the proportionality of the sum frequency intensity to the square of the number density, N, of oscillators as indicated earlier. The smaller signal intensity is combined with a significantly greater noise level as compared to purely hydrogenated samples, possibly as the result of interfacial density fluctuations of the hydrogenated sample component within the sampled area. Reduced intermolecular interferences between oppositely oriented CH_2 groups mixed with CD_2 groups in adjacent hydrocarbon chains is a possible explanation for this observation if the smaller CH_3-SS/CH_2-SS ratios observed are meaningful. To test this possibility, we investigated 50/50 mixtures of *d*-C_{18}-PC/C_{18}-PC and *d*-C_{16}-PC/C_{16}-PC adsorbed at the interface. The C_{18} mixtures would be expected to give a relatively small CH_2-SS intensity regardless of intermolecular interferences and gave ratios within the error bar for results obtained from the purely hydrogenated C_{18}-PCs. The SF signal intensities measured from the C_{16}-PC mixtures were very small and noisy. These results unfortunately did not provide further insight into the adsorbed binary mixtures of C_{16}- and C_{18}-PCs. It is also not clear whether intermolecular interferences between oppositely oriented CH_2 groups within the sample layers significantly impact these VSFG measurements of hydrocarbon chain ordering.

CONCLUSIONS

Distinct differences in interfacial layer ordering of adsorbed symmetric chain PCs were observed as a function of chain length at an aqueous–CCl_4 interface. The C_{18}- and longer chain PCs were seen to form extremely well-ordered interfacial layers with chains in a predominantly all trans conformation, while C_{16}- and C_{15}-PCs formed layers with disordered chains. The C_{17}-PCs produced layers with an intermediate degree of order. These results are in contrast to those reported for interfacially adsorbed alkyl sulfonate monolayers at a similar interface in which increasing chain disorder was noted as a function of increasing length of the component hydrocarbon chains as attributed to a greater number of gauche conformers.[45] This indicates that the behavior of PCs adsorbed at a liquid–liquid interface is not determined mainly by chain solvation forces. We might reasonably expect such differences in molecular

packing arrangements between relatively simple charged surfactants displaying interhead group repulsion and the structurally more complicated zwitterionic PCs. Mixtures of C_{16}- and C_{18}-PCs adsorbed at the liquid–liquid interface exhibited a systematic increase in chain ordering as a function of the C_{18}-PC mole fraction that is representative of compositional alterations in membrane structure that are biologically needed to control membrane function.

The authors thank Dr. R. A. Walker for helpful discussions.

REFERENCES

1. Handa, T.; Saito, H.; Miyajima, K. Biochemistry 1990, 29, 2884–2890.
2. Miller, K. W.; Small, D. M. In Plasma Lipoproteins; Gotto, A. M. J., Ed.; Elsevier: New York, 1987; p 1–75.
3. Schumaker, V.; Lembertas, A. In Molecular Genetics of Coronary Artery Disease. Candidate Genes and Processes in Atherosclerosis; Lusis, A. J., Rotter, J. I., Sparkes, R. S., Eds.; Karger: New York, 1992; p 98–139.
4. Kakiuchi, T.; Kotani, M.; Noguchi, J.; Nakanishi, M.; Senda, M. J Colloid Interface Sci 1992, 149, 279–289.
5. Kakiuchi, T. In Liquid–Liquid Interfaces: Theory and Methods; Volkov, A. G., Deamer, D. W., Eds.; CRC Press: Boca Raton, FL, 1996; p 317–331.
6. Shchipunov, Y. A.; Kolpakov, A. F. Adv Colloid Interface Sci 1991, 35, 31–138.
7. Mingins, J.; Stigter, D.; Dill, K. A. Biophys J 1992, 61, 1603–1615.
8. Ogino, K.; Onishi, M. J Colloid Interface Sci 1981, 83, 18–25.
9. Mingins, J.; Taylor, J. A. G.; Pethica, B. A.; Jackson, C. M.; Yue, B. Y. T. J Am Chem Soc Faraday Trans 1 1982, 78, 323–339.
10. Redgrave, T. G.; Rakic, V.; Mortimer, B.-C.; Mamo, J. C. L. Biochim Biophys Acta 1992, 1126, 65–72.
11. Dill, K. A.; Stigter, D. Biochemistry 1988, 27, 3446–3453.
12. Stigter, D.; Dill, K. A. Langmuir 1988, 4, 200–209.
13. Smiley, B. L.; Richmond, G. L. J Phys Chem 1999, 103, 653.
14. Thoma, M.; Möhwald, H. J Colloid Interface Sci 1994, 162, 340–349.
15. Möhwald, H.; Dietrich, A.; Böhm, C.; Brezesinski, G.; Thoma, M. Mol Membr Biol 1995, 12, 29–38.
16. Ishida, H.; Iwatsu, K.; Kubota, J.; Wada, A.; Domen, K.; Hirose, C. J Chem Phys 1998, 108, 5957–5964.
17. Bain, C. D. J Chem Soc Faraday Trans 1995, 91, 1281–1296.
18. Guyot-Sionnest, P.; Hunt, J. H.; Shen, Y. R. Phys Rev Lett 1987, 59, 1597–1600.
19. Hirose, C.; Akamatsu, N.; Domen, K. J Chem Phys 1992, 96, 997–1004.
20. Hunt, J. H.; Guyot-Sionnest, P.; Shen, Y. R. Chem Phys Lett 1987, 133, 189–192.
21. Zhang, D.; Gutow, J.; Eisenthal, K. B. J Phys Chem 1994, 98, 13729–13734.
22. Conboy, J. C.; Messmer, M. C.; Richmond, G. L. J Phys Chem B 1997, 101, 6724–6733.
23. Walker, R. A.; Conboy, J. C.; Richmond, G. L. Langmuir 1997, 13, 3070–3073.
24. Bell, G. R.; Bain, C. D.; Ward, R. N. J Chem Soc Faraday Trans 1996, 92, 515–523.
25. Du, Q.; Superfine, R.; Freysz, E.; Shen, Y. R. Phys Rev Lett 1993, 70, 2313–2316.
26. Bloembergen, N.; Lee, C. H. Phys Rev Lett 1967, 19, 835–837.
27. Bloembergen, N.; Simon, H. J.; Lee, C. H. Phys Rev 1969, 181, 1261–1271.
28. Löbau, J.; Wolfrum, K. J Opt Soc Am B 1997, 14, 2505–2512.
29. Conboy, J. C.; Messmer, M. C.; Richmond, G. L. J Phys Chem 1996, 100, 7617–7622.
30. Walker, R. A.; Gruetzmacher, J. A.; Richmond, G. L. J Am Chem Soc 1998, 120, 6991–7003.
31. Akamatsu, N.; Domen, K.; Hirose, C. J Phys Chem 1993, 97, 10070–10075.
32. Wolfrum, K.; Laubereau, A. Chem Phys Lett 1994, 228, 83–88.
33. Smiley, B. L.; Walker, R. A.; Gragson, D. E.; Hannon, T. E.; Richmond, G. L. SPIE 1998, 3273, 134–144.
34. Sun, W.-J.; Tristram-Nagle, S.; Suter, R. M.; Nagle, J. F. Biophys J 1996, 71, 885–891.
35. Tsai, Y.-S.; Ma, S.-M.; Kamaya, H.; Ueda, I. Mol Pharmacol 1987, 31, 623–630.
36. Suezaki, Y.; Shibata, A.; Kamaya, H.; Ueda, I. Biochim Biophys Acta 1985, 817, 139–146.
37. Lin, H.-C.; Ueda, I.; Lin, S. H.; Shieh, D. D.; Kamaya, H.; Eyring, H. Biochim Biophys Acta 1980, 598, 51–65.
38. Finegold, L.; Singer, M. A. Biochim Biophys Acta 1986, 855, 417–420.
39. Sun, W.-S.; Tristram-Nagle, S; Suter, R. M; Nagle, J. F. Biochim Biophys Acta 1996, 1279, 17–24.
40. Snyder, R. G.; Liang, G. L.; Strauss, H. L.; Mendelsohn, R. Biophys J 1996, 71, 3186–3198.
41. Rowe, E. S. Biochemistry 1987, 26, 46–51.
42. Chiou, J.-S.; Kuo, C.-C.; Lin, S. H.; Kamaya, H.; Ueda, I. Alcohol 1991, 8, 143–150.
43. Yeagle, P., Ed. The Structure of Biological Membranes; CRC Press: Boca Raton, FL, 1992.
44. Garidel, P.; Blume, A. Biochim Biophys Acta 1998, 1371, 83–95.
45. Conboy, J. C.; Messmer, M. C.; Richmond, G. L. Langmuir 1998, 14, 6722.